Available online at www.sciencedirect.com
ScienceDirect
Scripta Materialia 63 (2010) 597–600
Scripta MATERIALIA
www.elsevier.com/locate/scriptamat

Properties of porous multi-layered free-standing ceramic microchannels

Zdeněk Chlup[a,*] and David Salamon[b]

[a]Institute of Physics of Materials, Academy of Sciences of the Czech Republic, Zizkova 22, 616 62, Brno, Czech Republic
[b]Membrane Technology Group, University of Twente, P.O. Box 217, 7500 AE Enschede, The Netherlands

Received 16 April 2010; revised 31 May 2010; accepted 1 June 2010
Available online 4 June 2010

Preparation of porous microtubular materials has attracted growing interest in recent decades. The free-standing microchannels investigated here were prepared by the microtemplating method, which allows the preparation of a multilayered material from a single suspension. The mechanical properties were characterized using the three-point flexural test and the tension test. The results present the possibility of significantly reducing the influence of structural defects by the formation of a single ceramic multi-layered structure via repeated deposition of thin monolayers.

Keywords: Microchannels; Flexural test; Tension test; Layered structures

Ceramic porous structures have potential for applications as critical components in many industrial applications. Ceramic materials have several desired properties that are important for microfluidic systems, e.g. heat resistance, hardness and corrosion resistance. Porous alumina is widely used in membrane technology as a ceramic support [1] or directly as the membrane [2]. Decreasing the diameter of ceramic hollow fibres brings the advantages of ceramic materials to microtechnology. The alumina microcomponents were produced by a rapid prototyping process chain and subsequently assembled to ceramic microheat exchangers [3]. The steam reforming of hydrocarbon fuels is a promising method that uses ceramic microreactors for the production of hydrogen as portable electrical power sources. Additionally, the demonstrated stability of these ceramic microreactors at high temperatures in the presence of oxygen and steam makes them promising for other high-temperature reactions occurring under harsh chemical conditions, such as the partial oxidation of hydrocarbons [4]. In addition to the above-mentioned functional requirements, additional conditions have to be fulfilled. Adequate mechanical properties are essential for such microstructure. The requirement of relatively high porosity governed by the functionality goes against the high strength required by free-standing self-supporting microchannel structures. The mechanical loading is high because not only gases but also liquids are used. The initial fluid flow through the microchannel causes additional mechanical stresses in pores in the form of capillary forces.

The microtemplating technique was used in this work to prepare porous multilayered free-standing alumina microchannels. The controlled dip-coating of a sacrificial polymeric fibre template with suspensions containing sinterable particles is the basis for the microtemplating method. The template is sacrificed during the subsequent firing stage.

A suspension containing pure α-alumina powder (AKP 15, $d_{50} = 0.61$ μm, Sumitomo Chemical Co. Ltd., Japan) was prepared by adding 52.8 wt.% alumina (AKP-15 powder) to 40.7 wt.% 2-propanol enriched by 1.9 wt.% dispersant (Solperse 20,000, Noveon, England), followed by deagglomeration of the powder in a ball mill (5 mm zirconia balls) for 2 h. Afterwards 3.5 wt.% binder (Polyvinyl Butyral, B-98) and 1.1% plasticizer (Butyl Benzyl Phthalate, S-160) were gradually added and consequently ball-milled for 48 h. The prepared suspension was used for multiple dip-coating of a polypropylene fibre (porous and hollow internal structure, outer diameter 300 μm) and a polyimide fibre (porous and hollow internal structure, outer diameter 970 μm). The velocity of the fibres withdrawing from the suspension was a constant 4.8 mm s^{-1}. The porous alumina multi-layered ceramic free-standing microchannels were prepared by sintering at 1400 °C for 4 h and the procedure took place in air. The microchannels prepared by five coatings of the

* Corresponding author. Tel.: +420 532290335; e-mail: chlup@ipm.cz

1359-6462/$ - see front matter © 2010 Acta Materialia Inc. Published by Elsevier Ltd. All rights reserved.
doi:10.1016/j.scriptamat.2010.06.001

polypropylene fibre were named D05 and the nominal outer diameter was 0.5 mm after sintering. The microchannels prepared by eight coatings of the polyimide fibre were denoted D15 and the nominal outer diameter was 1.5 mm after sintering.

The mechanical properties were characterized using both the three-point flexural test and the tension test, and the modified testing methodology developed previously for characterization of ceramics foam structures [5] was adopted. At least five valid tests were conducted for each data set and statistically evaluated.

A three-point flexural test configuration was used with a span of 16 mm. The loading of 20 mm long specimens was realized using an Instron 8862 (Instron, USA) testing system. A typical crosshead speed of 1.66 μm s^{-1} was applied and a precise inductive extensometer (resolution below 1 μm) was employed to measure the deflection.

Tensile properties were characterized on specimens with a total length of 50 mm and both ends were glued into tubular holders. The specimens and their holders were placed into loading grips, which allow free movement in two axes to guarantee pure uniaxial loading. A Zwick Z50 (Zwick/Roell, Germany) testing machine with a 1 kN load cell was used for the loading. Displacement was monitored using a non-contact 3D system Q-300 (Dantec Dynamics, Germany) based on electronic speckle pattern interferometry (ESPI) with a resolution of 100 nm. A crosshead speed of 0.833 μm s^{-1} was used in order to ensure sufficient conditions for the ESPI measurement.

Image analysis was applied for shape and dimension measurements. Due to the rather complicated and non-uniform profile of the microchannels it was necessary to simplify the calculation of the loaded profile for the flexural strength determination. The model of a tube idealizing the real microchannel shape was used. The two limits of the outer diameter were measured by a circumscribed and an inscribed circle. The inner diameter was measured precisely as it was sufficiently regular. Based on these optical measurements, the flexural strength and flexural module of elasticity in the two limit situations were determined by the following formulas:

$$\sigma_{flex(j)} = \frac{4Fl^3}{3\pi(D_{(i)}^4 - d^4)D_{(i)}},$$

$$E_{flex(j)} = k\frac{4l^3}{3\pi(D_{(i)}^4 - d^4)},$$

where F is the maximum force, l is the span distance, D is the outer diameter, d is the inner diameter and k is the slope of the linear part of the deflection curve. The index i marks if the outer diameter is taken as a circumscribed ($i =$ max, $j =$ min) or an inscribed ($i =$ min, $j =$ max) circle. Index j indicates which limit is estimated.

The tensile strength was calculated as the maximum force divided by the area of the fractured specimens, which is the projection of the fracture surface onto the plane perpendicular to the loading axis. Elongation was calculated using the deformation map obtained from the ESPI measurement by the measuring the displacement between two points lying on the loading axis. The initial gauge length was 30 mm. Because of the high precision of the elongation measurement, it was also possible to estimate the Young's modulus of elasticity for D15.

An extensive fractography was conducted on the fracture surfaces using a Jeol 6460 scanning electron microscope (Jeol, Japan) and a Lext OLS3100 laser confocal microscope (Olympus, Japan). The open porosity was measured using Archimedes' principle (ASTM C373–88) and the microchannel volume was not taken into account.

The multi-coating and rapid drying procedure between coating steps formed a density gradient between the inner and outer surface of each layer. These density gradients create sections in the profile of the sintered microchannels (see Fig. 1). The porosity changes are very local, with porosity only appearing in the very thin surface layer that was exposed to air during the drying procedure. Sintered free-standing alumina microchannel structures contain five and eight layers inside samples D05 and D15, respectively. The inner diameter of the designed microchannels is very regular for both D05 ($= 256 \pm 2$ μm) and D15 ($= 850 \pm 11$ μm). The average thickness of the porous wall (38% of the open porosity) is 122 and 325 μm for D05 and D15, respectively.

The flexural strength determination seems to be an easy way to describe the mechanical behaviour of microchannels. The specimen preparation is simple to conduct and the testing setup is also commonly used for ceramic material testing. Table 1 summarizes the experimental values of flexural strength and estimated flexural modulus of elasticity. The flexural strength exhibits minimal values of 300 MPa for both types of microchannel, which meets the requirement of applications in severe conditions.

However, the results overestimate the fracture resistance of the microchannel due to the nature of the flexural strength test in which the maximum stress is only imposed in the outer thread of the tube. This fact, as well as the correctness of the applied approach to

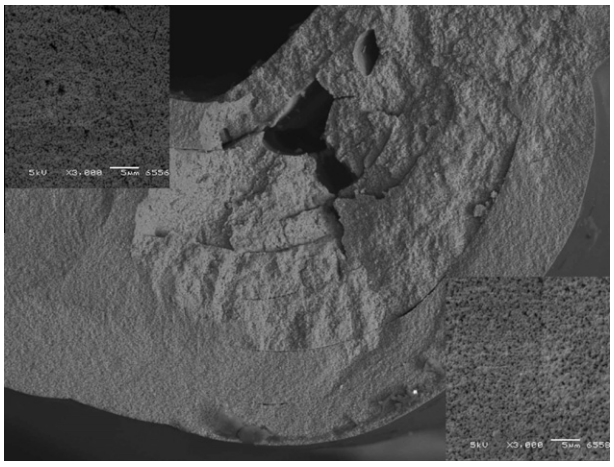

Figure 1. Scanning electron microscope microstructures of sintered sample D15: cross-section with eight layers, inner surface with high porosity (up), outer surface with low porosity (down).

Table 1. Flexural strength and module of elasticity determined from the three-point bend test.

Microchannel type	$\sigma_{flex(\min)}$ (MPa)	$\sigma_{flex(\max)}$ (MPa)	$E_{flex(\min)}$ (GPa)	$E_{flex(\max)}$ (GPa)
D05	277 ± 79	416 ± 110	103 ± 20	179 ± 35
D15	302 ± 32	428 ± 24	179 ± 29	279 ± 18

Table 2. Tensile strength and Young's modulus.

Microchannel type	R_m (MPa)	E (GPa)
D05	53 ± 23	-
D15	90 ± 20	310 ± 30

simplify the loaded profile, were confirmed by a numerical calculation using a finite element method. The idealized specimen geometry and elastic properties determined by the tensile test were implemented in the numerical model. The tube was loaded in the same way as in the experiment up to the maximum deflection corresponding to fracture. The result of the maximum principal stress obtained numerically on the outer diameter was 362 MPa, which corresponds well with the experimentally determined flexural strength values. The analyzed microchannels have a graduated porosity from the inner to the outer surface that was created by the controlled deposition of five or eight different thin layers. The properties of this functionally graduated material vary from the inner to the outer surface of each layer. Additionally the flexural strength is dependent on the surface quality. Therefore, the flexural strength values reflect the properties of the outer layer of the microchannels.

Results that are more relevant for application design purposes can be expected by uniaxial tensile loading. However, difficulties in gripping this fragile, small test piece as well as perfect load transfer and alignment have to be overcome. The solution is to transfer load by fixing 10 mm of the sample ends into tubular holders using epoxy glue. The typical loading curve obtained from the tension test of the microchannel is displayed in Figure 2 (left), together with an example of the deformation map obtained by the ESPI technique just before the fracture (Fig. 2, right).

The results obtained from the tension tests are presented in Table 2, where average values and corresponding standard deviations are shown. In order to eliminate the possible effect of gripping, only specimens in which the fracture occurred in the middle part were used for the characterization. The tensile strength is significantly lower than the flexural strength. This difference can be partially explained by taking into account different loaded volumes at each testing approach, which gives statistically different chances of finding a defect for the fracture initiation. The Weibull approach is suitable if the presence of a weakest link fracture mechanism is assumed [6]. The application of this approach allows the comparison of strength characteristics between different loading configurations by taking into account the effectively loaded volume. The Weibull modulus $m = 3.5$ was determined from tensile strength values and was further used to calculate the effective volume using the gamma function. The three-point flexural specimens had an effective volume only 0.8% of the effective volume of the tensile specimen. The calculated theoretical strength ratio between the flexural and tensile strength (using Weibull's approach) is 4, but the measured ratio is between 5 and 8. This means that the surface quality of the outer layer, which evidently contains smaller defects than the layer volume, and the gradually changing microstructure within one layer also played important roles.

Figure 3 shows micrographs of the fracture surface (top view) of a fractured specimen at flexure (left) and tension (right). The arrows indicate the direction of crack propagation, which is given by the loading conditions in the case of flexure and determined on the basis of the fracture pattern in the case of tension. The visible increase in fracture relief at the top-left corner of the tensile specimen is partially caused by changing the local stress conditions from uniaxial to triaxial. Additionally, the crack velocity declines during crack propagation due to a reduction in available elastic energy, and therefore the fracture pattern is changed from smooth to relatively

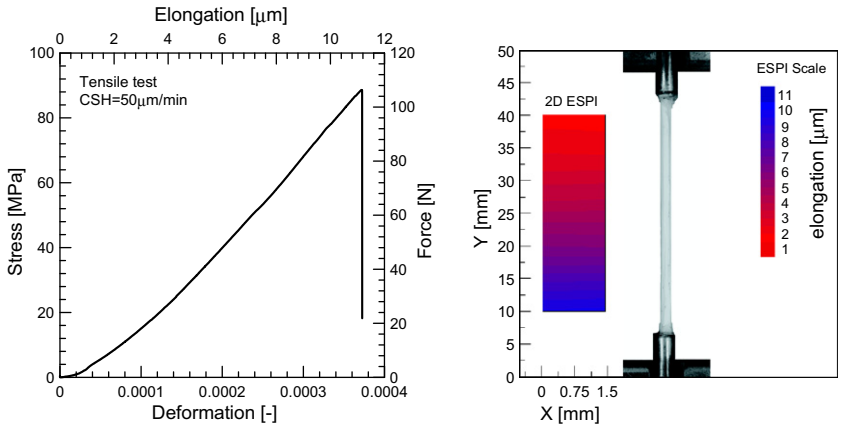

Figure 2. An example of the force–elongation trace of a tensile test and a deformation map obtained by the ESPI technique corresponding to the fracture point.

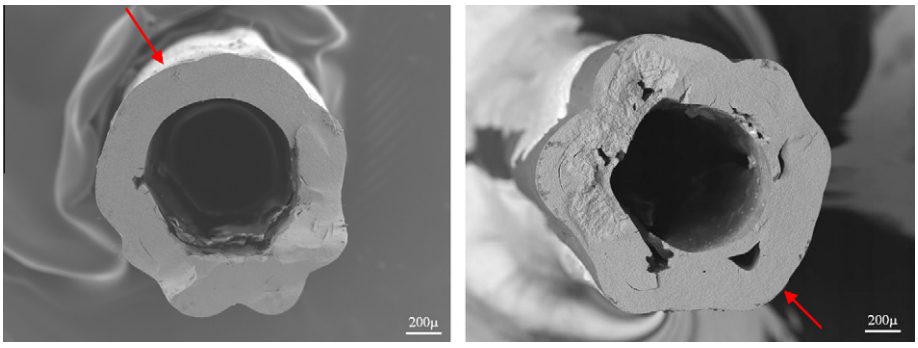

Figure 3. The fracture surface of specimen D15 loaded in three-point bending (left) and tension (right).

rough. From both micrographs it is obvious that the layered structure is irrelevant in the initial stages of the crack propagation. A detectable influence can be found, however, during the final fracture stage. The fracture surface in Figure 3 (left) shows a significant deflection of the main crack, which was mainly caused by the non-correspondence of the planes of maximal stress and crack initiation. In contrast, the specimen loaded in tension exhibited a flat fracture surface perpendicular to the loading axis. Only negligible signs of the laminate structure are observable near large pores, which change the local stress conditions in the fracture surface of the tensile-loaded specimen.

The preparation of a layered structure has brought one advantage over existing methods which use a one-step procedure. Free-standing microchannel structures are very sensitive to any processing errors due to the small wall thickness. The multi-layered structure partially eliminates this sensitivity because it limits the size of defects to the thickness of one layer. This also explains why the measured flexural strength values are significantly greater than the values reported in the literature [7–8].

In conclusion, the characteristics of flexural and tensile strength) of free-standing multilayer microchannels with two different dimensions were determined, together with their elastic properties (module of elasticity. The flexural strength was determined within a range due to the irregular geometry of the outer diameter. Both types of microchannel exhibit similar flexural strength at a level of 300 MPa. However, the scatter is significantly higher for D05, because of the greater influence of processing defects (less layers in the structure).

Tensile strength was established to be 50 MPa for D05 and 90 MPa for D15. The tensile strength scatter was similar in both cases. The influence of processing defects was reflected in the strength values but not in the scatter. However, the tensile strength was significantly (at least threefold) lower than the values obtained by flexure. This fact led to the conclusion that the flexural test is not suitable for strength characterization because it takes into account mainly the outer surface layer. This is also supported by conducted statistical analysis taking into account the effectively loaded volume. The average values of the elasticity module show opposite trends to the strength values with analogous scatter.

Fractographic analysis revealed that the layered structure played an insignificant role in crack propagation during the tension test and therefore the microchannel can be modelled as a monolithic material with a porosity gradient. On the other hand, the layered structure has a significant influence on the distribution and size of processing defects in the sintered ceramic structure. The presence of large strength-limiting defects has a low probability due to the small dimensions of the layers. Accordingly, the multi-layered structure enhances the reliability of the microchannels.

The authors gratefully acknowledge the financial support of project Nos. M100410902 and GA101/09/1821, and the Dutch Technology Foundation (STW).

[1] H. Verweij, J. Mat. Sci. 38 (2003) 4677–4695.
[2] R. Del Colle et al., J. Membrane Sci. 289 (2007) 58–66.
[3] B. Alm et al., Chem. Eng. J. 135 (2008) S179–S184.
[4] Christian et al., J. Catal. 241 (2006) 235–242.
[5] L. Rehorek et al., Ceramics – Silikáty 53 (4) (2009) 237–241.
[6] G.D. Quinn, J. Am Ceram. Soc. 86 (2003) 475–479.
[7] R. Melcher et al., Materials Letters 60 (2006) 572.
[8] D. Coimbra et al., Journal of Materials Science 35 (2000) 3347.